Available online at www.sciencedirect.com

ScienceDirect

Procedia Materials Science 3 (2014) 1922 – 1927

Procedia Materials Science

www.elsevier.com/locate/procedia

20th European Conference on Fracture (ECF20)

Engineering criterion for rupture of brittle particles in a ductile matrix including particle size and stress triaxiality effects

Andrew Abu-Muharib[a,b]*, Andrey P Jivkov[a], Peter James[b]

[a]*Mechanics of Physics of Solids Research Team, Modelling and Simulation Centre, School of Mechanical Aearospace and Civil Engineering, The University of Manchester, M13 9PL, UK*

[b]*AMEC – Clean Energy Europe, Birchwood, Risely, Warrington, UK*

Abstract

Catastrophic failure due to cleavage fracture is caused by the rapid propagation of a micro-crack in the vicinity of a macroscopic flaw. Micro-cracks are initiated at second-phase brittle particles, present in the steel in different sizes and distributed randomly in the volume. The current understanding is that such particles rupture when overloaded by the plastically deforming matrix. To predict the experimentally observed statistical nature of cleavage fracture under different constraint conditions, it is pertinent to develop a particle size and constraint dependent criterion for the failure of a brittle particle in a ductile matrix.

In this work the failure energy of an elastic-brittle spherical particle in a ductile matrix is analysed. Several loading conditions were examined, from constrained-uniaxial through to plane strain with varying levels of constraint. To develop a size dependent condition, results for multiple particle radii were investigated within a fixed matrix volume. The particle and matrix were deformed initially; subsequently nodes along the particle mid-plane were released progressively imitating crack opening. The energy associated with particle rupture was determined from the change in reaction force before and after release and corresponding opening displacements.

The results for each loading case show clear linear relation between rupture energy and particle size. Further the results show the dependence of rupture energy on constraint, with a distinct increase of failure probability with increasing constraint. Finally, an expression for particle rupture dependence on size, stress triaxiality, and plastic strain level is derived. It is intended that this model will then be used to advance continuum-based local approach models to cleavage and meso-scale models for distributed interacting micro-cracks.

Selection and peer-review under responsibility of the Norwegian University of Science and Technology (NTNU), Department of Structural Engineering

* Corresponding author. *E-mail address:* andrew.abu-muharib@manchester.ac.uk

Selection and peer-review under responsibility of the Norwegian University of Science and Technology (NTNU), Department of Structural Engineering
doi:10.1016/j.mspro.2014.06.310

Keywords: micromechanical; length-scale; rupture-criterion; cleavage fracture

1. Introduction

Safety assessment and life extension decisions in nuclear power plants require reliable approaches for predicting changes in cleavage fracture toughness behavior of ferritic RPV steels due to irradiation and defect location effects. Cleavage failure of ferritic steels is a mechanistic process, activated by the rupture of brittle second phase particles such as carbides which are distributed randomly throughout the ductile plastically deforming matrix. Brittle failure of these second phase particles is caused by local overloading due to the re-distribution of stresses by plastic-deformation of the surrounding matrix (Hahn 1984; McMahon & Cohen 1965; Gurland 1972). Hence limiting the region where micro-cracks are formed to the plastic zone ahead of a macroscopic flaw.

Local approaches (LA) to cleavage fracture could account for the micro-mechanisms involved in the failure phenomenon, including the nucleation of micro-cracks at second phase brittle particles and the propagation of a critical micro-crack which may lead to component failure (Pineau 2006). The original Beremin LA model (Beremin et al. 1983) is based on two main assumptions: that the global failure probability is a weakest-link event and that the individual failure probabilities are dictated by local mechanical fields and associated microstructure data, such as the size distribution and number density of cleavage-initiating particles. This work aims to explore this particle size dependency, whilst accounting for both the effects of variation in plastic strain and stress triaxiality conditions, to provide an updated energy criterion for rupture. From this energy based criterion a future particle failure probability function will feed directly into existing LA models, such as that developed by Jivkov (Jivkov et al. 2011). It can also be used to influence micromechanical data for probability of failure of particles in an elastic-plastic system to advance a proposed micro-crack interaction model (Abu-Muharib et al. 2013).

Nomenclature

$\varepsilon_{11}/\varepsilon_{22}$	triaxiality, applied constraint ratio
ε^{p}_{22}	plastic strain applied to model
ε_{ii}	strain, ii subscript denotes corresponding model direction
$G_{rupture}$	initiating rupture energy of particle fracture (J/m^2)
$G_{material}$	matrix material energy parameter (J/m^2)
G	$G_{rupture}/G_{material}$
R	particle radius
rf_{22}	reaction forces at particle nodes released
u_{22}	nodal displacements of particle

2. Modelling methodology

2.1. Brittle particle – ductile matrix representation

To capture the required micromechanical behavior of a brittle particle within a ductile, plastically deforming matrix, a quarter geometric representation of a finite cubic solid surrounding a sphere was modelled using the FE analysis code ABAQUS 6.10. The surrounding cubic (20Lx20Lx20L), where L is the largest particle radius, matrix was used to transmit the applied elastic-plastic loads to a range (R=0.1→1.0) of different particle radii (see Figure 1). Material properties attributed to the modelling methodology are shown in Table 1, with elastic-perfectly plastic and elastic-brittle material behaviors applied to the ferritic steel matrix and carbide particle respectively. Controlled

displacements (ε_{22} = 0.005, 0.01, 0.02, 0.04, 0.05, 0.06) were applied along the y-axis depicting plane strain conditions (ε_{33} = 0) and to model several resultant plastic strain states. The applied displacements equated as 0.5-6% total strain of the overall model volume, the upper bound of which is typically seen for catastrophic cleavage events in ferritic steels. In order to consider to the effect of triaxiality on particle failure several constraint cases ($\varepsilon_{11}/\varepsilon_{22}$ = 0.0, 0.2, 0.4, 0.6, 0.8 and 1.0) were also applied to each of the displacement conditions described.

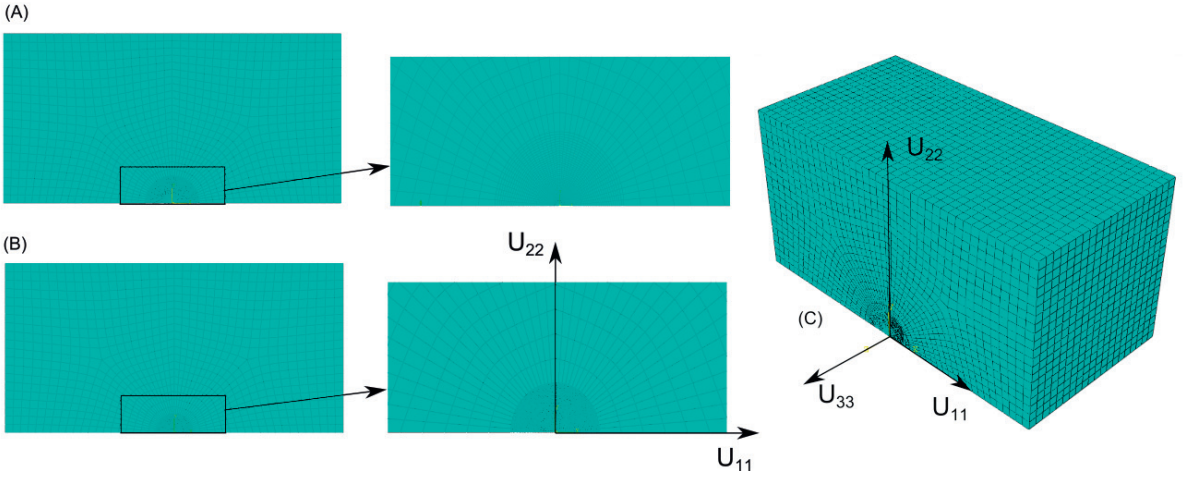

Figure 1. Meshed models of FE analysis: (A) schematic of model with carbide radius R = 1.0, (B) schematic of model with carbide radius R = 0.1 and (C) 3D schematic representation of FE model.

2.2. Brittle particle rupture energy model

Two stage FE models were developed for each of the conditions and particle radii described in section 2.1. During the primary phase, relevant plane strain boundary conditions were initiated and associated displacements applied. Relevant data was collected from the first step; most importantly this included the reaction forces, rf_{22}, at the particle mid-plane. At the second step the nodes defining the particle mid-plane, at the lower Y-axis face of the model, were released from the previous constrained boundary condition. All other boundary conditions and displacements were maintained. This phase simulated particle rupture to provide the rupture energy, captured from the corresponding particle node displacements, u_{22}, and previously described reaction forces, rf_{22}.

Furthermore, a separate solid cubic model, of the same dimensions, material properties and under the same loading conditions, but without the particle inclusion was developed representing the ductile plastically deforming matrix. This served to deliver relevant necessary data to normalise results within the main modelling strategy and to provide a quantitative measure of the mechanical response of the matrix.

Table 1. Material input parameters for simulations

Material	Elastic modulus *E* (GPa)	Poisson's ratio ν	Yield stress σ_Y (MPa)
Ferritic Steel	200	0.3	600
Carbide	400	0.19	-

3. Results and discussion

3.1. Rupture energy dependency – particle size

Previously, a cubic dependence of failure probability on particle size (Wallin et al. 1984) has been suggested on the base of fiber-load model. With the model presented here an initial work was carried out showing that the stress-state through the particle followed an R^3 dependency under unconstrained uniaxial conditions. However, it did not hold for a change in applied loading conditions and the stress-state through each particle radii proved indistinguishable, thus it was necessary to change from a stress based criterion to an energy criterion. The modelling methodology employed captured energy changes for the various different cases simulated. Results from the simulations infer that the initiating rupture energy criterion for an elastic-brittle particle in a ductile plastically deforming matrix can be described as a function of particle radius R, applied plastic strain ε^p_{22} and simulated triaxiality effects $\varepsilon_{11}/\varepsilon_{22}$. To help process the results $G_{rupture}$ was normalised using $G_{material}$, proposed to be 1MPa, although this value needs further examination and is proposed to be a material dependent property, considered to be beyond the scope of this work at this current time. Most significantly a linear relationship can be seen from Figure 2, between $G_{rupture}$ and the particle radii. This relationship holds for all cases examined under different constraint variations and applied plastic strain conditions. Moreover, this linear function is separable from the constraint and plastic strain effects as discussed in the following subsections.

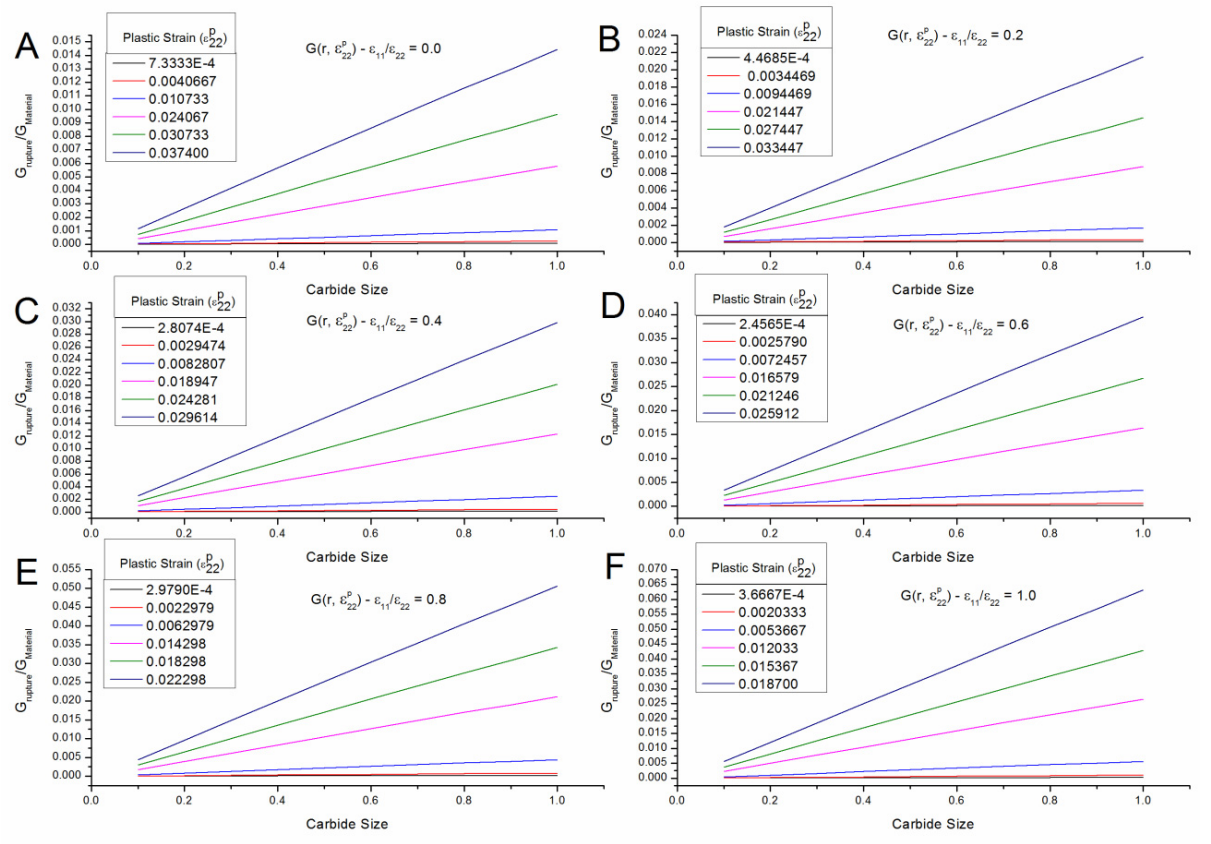

Figure 2. Relationship between initiating rupture energy and particle radius for a range of plastic strains under the following constraint cases: (A) $\varepsilon_{11}/\varepsilon_{22} = 0.0$, (B) $\varepsilon_{11}/\varepsilon_{22} = 0.2$, (C) $\varepsilon_{11}/\varepsilon_{22} = 0.4$, (D) $\varepsilon_{11}/\varepsilon_{22} = 0.6$, (E) $\varepsilon_{11}/\varepsilon_{22} = 0.8$, (F) $\varepsilon_{11}/\varepsilon_{22} = 1.0$.

3.2. Rupture energy dependency – plastic strain

Figure 2 shows that for the same triaxiality conditions, and under increasing applied ε^{p}_{22}, there was a significant increase in the particle rupture energy $G_{rupture}$. This trend followed for each of the constraint cases examined and is to be expected, given that plastic overload is needed to for carbide rupture and subsequent cleavage fracture conditions to occur. Figure 3 is a curve fitting analysis taken from the separate linear functions seen for different ε^{p}_{22} conditions seen in Figure 2. It shows that the $G_{rupture}$ has a power dependency on ε^{p}_{22} and, under the material parameters used in this model, is a square function. This means that the plastic strain contribution can be separated to be $G_{rupture} \rightarrow C_1(\varepsilon^{p}_{22})^2$, with a scaling coefficient, C_1, that has been included.

3.3. Rupture energy dependency – plastic strain

It was found that the coefficient, C_1, presented in section 3.2, may be attributed to the material dependent behavior with varying triaxiality. As shown in Figure 2, increasing the level of constraint saw a universal increase in $G_{rupture}$, for one and the same particle radius, yet varying plastic stain levels were produced under the same applied displacement. Thus it followed that this trend could be separated from both the carbide radius and plastic strain functions. Analysis of this coefficient found that it fitted an exponential function with two defined parameters; an exponent rate of change and initial offset value to account for $\varepsilon_{11}/\varepsilon_{22} = 0$. There was still some material property dependency, in the form of a separate fixed coefficient, C_2. Here, for the selected material, C_2 was found to have a value of 10.99. The final function describing the stress triaxiality conditions in relation to initiating particle rupture energy was found to be fitted by $G_{rupture} \rightarrow C_2\,(e^{2.8(\varepsilon 11/\varepsilon 22)} - 0.033)$.

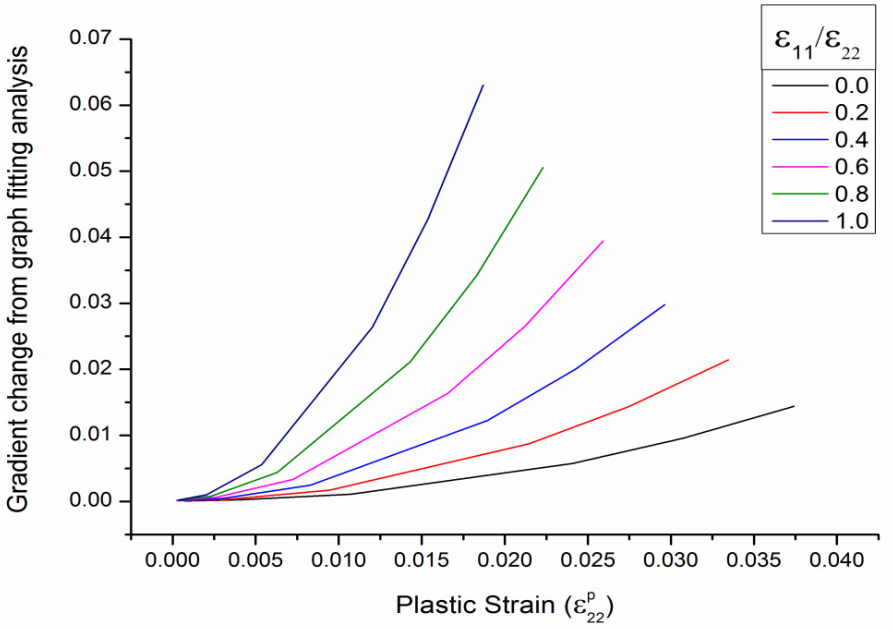

Figure 3. Curve fitting analysis of plastic strain (ε^{p}_{22}) variable for different constraint ($\varepsilon_{11}/\varepsilon_{22}$) cases.

4. Conclusion

This work presented in this paper includes a FE modelling methodology which has enabled an initiating rupture energy criterion to be defined for a brittle-elastic particle in a surrounding ductile, plastically deforming matrix. Simulated conditions accounted for variations in particle size, plastic strain and stress triaxiality. The proposed energy criterion including all terms is shown in Equation 1 below. This is formed from the separable functions for particle size, plastic strain and stress triaxiality.

$$G = C_2\left(\exp^{2.8(\varepsilon_{11}/\varepsilon_{22})} - 0.033\right)\cdot\left(R\right)\cdot\left(\varepsilon_{22}^{P}\right)^2 \quad (1)$$

The function follows current ideology, by predicting increases in rupture energy and subsequently failure probability for increasing particle size. However, it is inferred that this is a linear dependency for the plane strain conditions considered, rather than the previously thought cubic dependency on particle size. Furthermore, the effects of increased triaxiality and plastic overloading were found to have an increased effect on particle failure. This is also in line with current understanding, where it was possible to successfully separate their contributions into exponential and power functions, respectively.

Future work is needed to capture the effects on the coefficients C_1 and C_2 with changes to material properties. It is also necessary to consider further analysis to confirm, or not, the power and exponential function fits over more material and loading conditions.

Acknowledgements

A. Abu-Muharib would like to acknowledge the support from EPSRC via the Nuclear EngD Doctoral Training Centre at The University of Manchester's Dalton Nuclear Institute and the ongoing support from sponsoring company AMEC – Clean Energy Europe.

References

Abu-Muharib, A. et al., 2013. Cleavage Fracture Modelling for RPV Steels: Discrete Model for Collective Behaviour of Micro-Cracks. In *ASME 2013 Pressure Vessels & Piping Division Conference*. Paris.

Beremin, F., Pineau, A. & Mudry, F., 1983. A local criterion for cleavage fracture of a nuclear pressure vessel steel. ... *transactions A*, 14(11), pp.2277–2287.

Gurland, J., 1972. Observations on the fracture of cementite particles in a spheroidized 1.05% C steel deformed at room temperature. *Acta Metallurgica*, 20(5), pp.735–741.

Hahn, G., 1984. The influence of microstructure on brittle fracture toughness. *Metallurgical and Materials Transactions A*, 15(6), pp.947–959.

Jivkov, A., Lidbury, D. & James, P., 2011. Assessment of local approach methods for predicting end-of-life toughness of RPV steels. In *Proceedings of the ASME 2011 Pressure Vessels and Pipes*. Baltimore, pp. 293–302.

McMahon, C. & Cohen, M., 1965. Initiation of cleavage in polycrystalline iron. *Acta Metallurgica*, 13(6), pp.591–604.

Pineau, a., 2006. Development of the Local Approach to Fracture over the Past 25 years: Theory and Applications. *International Journal of Fracture*, 138(1-4), pp.139–166.

Wallin, K., Saario, T. & Törrönen, K., 1984. Statistical model for carbide induced brittle fracture in steel. *Metal Science*, 18(January), pp.13–16.